Available online at www.sciencedirect.com
ScienceDirect
Biochimica et Biophysica Acta 1767 (2007) 660–665
Biochimica et Biophysica Acta
BBA
www.elsevier.com/locate/bbabio

Artificial model of photosynthetic oxygen evolving complex: Catalytic O_2 production from water by di-μ-oxo manganese dimers supported by clay compounds

Masayuki Yagi [a,c,*], Komei Narita [a], Syou Maruyama [a], Koji Sone [a,c], Takayuki Kuwabara [a,c], Ken-ichi Shimizu [b,1]

[a] Faculty of Education and Human Sciences, Niigata University, 8050 Ikarashi-2, Niigata 950-2181, Japan
[b] Graduate School of Science and Technology, Niigata University, 8050 Ikarashi-2, Niigata 950-2181, Japan
[c] Center for Transdisciplinary Research, Niigata University, 8050 Ikarashi-2, Niigata 950-2181, Japan

Received 25 September 2006; received in revised form 2 November 2006; accepted 6 November 2006
Available online 15 November 2006

Abstract

Adsorption of $[(OH_2)(terpy)Mn(\mu\text{-}O)_2Mn(terpy)(OH_2)]^{3+}$ (terpy=2,2′:6′,2″-terpyridine) (**1**) onto montmorillonite K10 (MK10) yielded catalytic dioxygen (O_2) evolution from water using a Ce^{IV} oxidant. The Mn K-edge X-ray absorption near edge structure (XANES) of the **1**/MK10 hybrid suggested that the oxidation state of the di-μ-oxo Mn_2 core could be Mn^{III}–Mn^{IV}. However the pre-edge peak in the XANES spectrum of **1** adsorbed on MK10 is different from the neat **1** powder. The kinetic analysis of O_2 evolution showed that the catalysis requires cooperation of two equivalents of **1** adsorbed on MK10. The reaction of the $[(bpy)_2Mn(\mu\text{-}O)_2Mn(bpy)_2]^{3+}$ (bpy=2,2′-bipyridine) (**2**)/MK10 hybrid with a Ce^{IV} oxidant evolved O_2. However, the turnover number value was less than unity for **2**/MK10, showing that **2** adsorbed on MK10 does not work as a catalyst. The terminal water ligands could be an important for the catalysis by adsorbed **1**. The mechanism of O_2 production by photosynthetic oxygen evolving complex is discussed based on catalytic O_2 evolution by **1** adsorbed on MK10.

Keywords: Oxygen evolving complex; Photosystem II; Manganese complex; Oxygen evolution; Water oxidation; Photosynthesis

1. Introduction

Water oxidation to evolve O_2 (Eq. (1)) is an important and fundamental chemical reaction in photosynthesis. This reaction is catalyzed by a unique manganese enzyme so-called oxygen evolving complex (OEC), whose active site is comprised of an oxo-bridged tetramanganese cluster including a calcium ion [1–6]. However, the mechanism of water oxidation by OEC is still a question under debate [4–6].

$$2H_2O \xrightarrow{OEC} O_2 + 4H^+ + 4e^- \quad (1)$$

O_2 evolution by synthetic manganese complexes as OEC models is important for providing experimentally proven key reactions for proposals of the water oxidation mechanism by OEC, and the several trailblazing works have been reported to give important key reactions [7–16]. However, clear demonstrations of catalytic O_2 evolution from water by synthetic manganese-oxo complexes had not been reported.

Several years ago, Limburg et al. reported that O_2 is evolved by the reaction of $[(OH_2)(terpy)Mn(\mu\text{-}O)_2Mn(terpy)(OH_2)]^{3+}$ (terpy=2,2′:6′,2″-terpyridine) (**1**) with the oxygen donor agent of NaClO or $KHSO_5$ in an aqueous solution [13,14]. The O–O bond was hypothesized to be formed by attack on the Mn^V=O by a hydroxide in O_2 evolution. However, the mechanism of the O_2 evolution is completely unclear, including even disproportionation of $2ClO^- \rightarrow O_2 + 2Cl^-$ which is known to be catalyzed by Mn^{II} and other Lewis acids [9]. Nevertheless, their works have triggered active research fields on syntheses, redox

* Corresponding author. Fax: +81 25 262 7151.
E-mail address: yagi@ed.niigata-u.ac.jp (M. Yagi).
[1] Present address, Department of Applied Chemistry, Graduate School of Engineering, Nagoya University, Chikusa-ku, Nagoya 464-8603, Japan.

0005-2728/$ - see front matter © 2006 Elsevier B.V. All rights reserved.
doi:10.1016/j.bbabio.2006.11.005

reactions, catalyses related to **1** and its derivatives [17–21]. Recently, Baffert et al. reported that electrochemical oxidation in an aqueous solution of **1** cannot produce O_2 [19].

We preliminary reported that the reaction of **1** with a Ce^{IV} oxidant leads to decomposition of **1** to MnO_4^- ions without O_2 evolution in an aqueous solution, whereas it produces O_2 catalytically from water when **1** is adsorbed on kaolin clay [21]. **1** adsorbed onto the heterogeneous clay matrix could be regarded as a functional model of OEC in which a manganese-oxo cluster located in a microscopically heterogeneous environment formed by proteins. The observation of O_2 evolution might shed light on the unsolved mechanism of O_2 production by OEC. Herein a **1**/montmorillonite K10 (MK10) hybrid is prepared to ensure the generality of O_2 evolution catalyzed by **1** adsorbed on heterogeneous clay matrixes, and evidence of catalytic O_2 production from water by adsorbed **1** on MK10. The similar di-μ-oxo Mn dimer $[(bpy)_2Mn(\mu\text{-}O)_2Mn(bpy)_2]^{3+}$ (bpy=2,2′-bipyridine) (**2**) was used as a control compound to discuss the mechanism of O_2 production. The kinetic data for kaolin systems in a preliminary report [21] are partially included to understand comprehensively the catalysis by **1** on heterogeneous clay matrixes. The mechanism of O_2 production by OEC will be discussed based on catalytic O_2 evolution by **1** adsorbed on MK10.

2. Materials and methods

2.1. Materials

$Mn(NO_3)_2$, $KMnO_4$, $Ce(NH_4)_2(NO_3)_6$ (Wako Pure Chemical Industries, Ltd.), terpy, bpy and MK10 (Aldrich Chemical Co. Inc.) were purchased and used without further purification.

2.2. Syntheses of *1*$(NO_3)_3$ and *2*$(ClO_4)_3$, and preparations of *1* and *2*/MK10 hybrids

1$(NO_3)_3$ was prepared by a procedure reported elsewhere [21]. **2**$(ClO_4)_3$ was synthesized according to the literature by Cooper [22]. These complexes were characterized by IR and UV-visible absorption spectroscopic measurements.

An aqueous solution (0–1.2 mM, pH=4.0) of **1** or **2** was added to an aqueous suspension (5–15 ml, pH=4.0) of MK10 (50–400 mg). The resulting suspension was filtrated after stirring for 30 min, and then dried under vacuum to yield a **1** or **2**/MK10 hybrid. The amount of **1** or **2** adsorbed was measured by the visible absorption spectral change of the aqueous solution before and after adding MK10.

2.3. Mn K-edge XANES measurements and O_2 evolution experiments

Mn K-edge X-ray absorption near edge structure (XANES) measurements were carried out in a transmission mode at BL-9A (Photon Factory in High Energy Accelerator Research Organization, Tsukuba, Japan) with a Si(111) double-crystal monochromator. The ionization chambers filled with N_2 for I_0 (17 cm) and N_2(85%)–Ar(15%) for I (31 cm) were used. High energy X-rays from high order reflections were removed by a pair of flat quartz mirrors coated with Rh/Ni that were aligned in parallel. The energy was defined by assigning the first inflection point of the Cu foil spectrum to 8980.3 eV. Normalization of XANES analysis was carried out using REX2000 (Rigaku, EXAFS analysis software). The adequate small portion of an aqueous solution (1.0 M) of a $Ce(NH_4)_2(NO_3)_6$ oxidant was added to the aqueous solution (pH=4.0) of **1** or **2** and to the aqueous suspension containing the **1** or **2**/MK10 hybrid. The reaction was typically followed in 2.0 ml of a liquid phase volume at pH=1.0 and 25 °C under the conditions of a large excess (50–100 mM) of Ce^{IV} vs. **1** or **2**. (The Ce^{IV} oxidant cannot work in solutions over pH=4. The pH of the solution changes to 1.0 by adding the Ce^{IV} solution.) The amount of O_2 evolved was analyzed using a Clark type oxygen electrode (Hansatech Instruments, Oxygraph OXYG1 and DW1/AD unit). Gas chromatograph (Shimadzu, GC-8A) equipped with a 5 Å molecular sieve column (argon carrier gas) was used to analyze the maximum O_2 amount evolved.

3. Results

When an aqueous solution of **1** was added to an aqueous suspension of MK10, **1** was adsorbed onto MK10 by cation exchange with Na^+. The adsorption isotherm of **1** onto MK10 is shown in Fig. 1, including kaolin data [23]. The concentration (w_{ads}/mol g^{-1}) of **1** adsorbed on MK10 rose up steeply at very low (almost zero) equilibrium concentrations (c_{eq}/M) of **1** in the solution, indicating the high adsorption equilibrium constant of **1** onto MK10. The maximum concentration ($(w_{ads})_{max}$=0.105 mmol g^{-1}) of **1** adsorbed onto MK10 was 5 times higher than that (0.022 mmol g^{-1}) for kaolin. These values are consistent with the cation exchange capacity of MK10 (0.35 meq g^{-1}) [24] and kaolin (0.02–0.15 meq g^{-1}) when the trivalent of a **1** cation is taken into account.

The Mn K-edge XANES spectrum of the **1**/MK10 hybrid is shown in Fig. 2, including those of a neat **1** powder and a $[(SO_4)(terpy)Mn^{IV}(\mu\text{-}O)_2Mn^{IV}(terpy)(SO_4)]$ [23] (**1a**) powder for comparison. It is well known that the Mn K-edge shifts to a high energy region by an increase in an oxidation state of Mn centers in a di-μ-oxo manganese dimer [25]. The near edge structure of the **1**/MK10 hybrid (w_{ads}=80 μmol g^{-1}) is closer to the neat **1** powder rather than the **1a** powder, suggesting that the adsorbed species possesses the di-μ-oxo Mn^{III}–Mn^{IV} core. However, the pre-edge peak around 6540 eV, assigned to a dipole forbidden 1s→3d transition of the Mn center, is different between the both, as shown in the magnified spectra in the range of 6535–6547 eV (inset of Fig. 2). The spectrum of neat **1** exhibited a pre-edge peak at 6539.3 eV, while the spectrum of

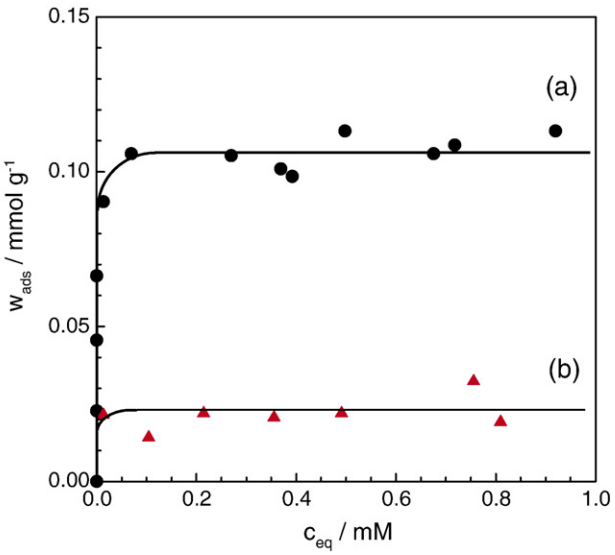

Fig. 1. Adsorption isotherms for adsorption of **1** onto (a) MK10 and (b) kaolin.

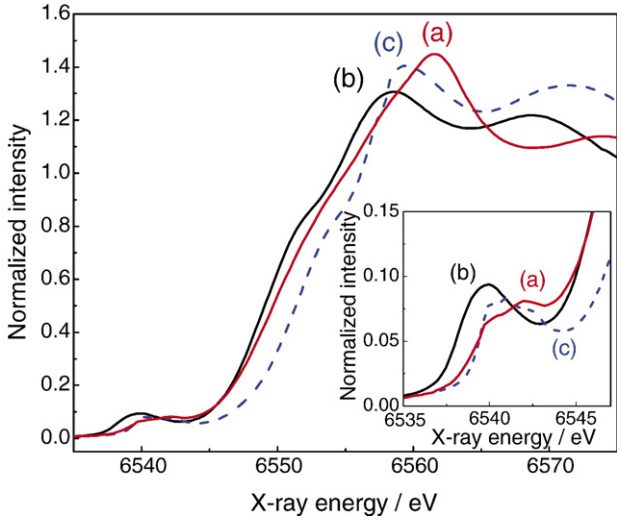

Fig. 2. Mn K-edge XANES spectra of (a) **1**/MK10 with w_{ads}=80 μmol g^{-1}, (b) **1** powder and (c) **1a** powder. The inset is the magnified spectra for the pre-edge peak around 6540 eV. The spectrum (c) was cited from reference 23.

the **1**/MK10 hybrid exhibited two separate pre-edge peaks at 6539.8 and 6542.2 eV. Pre-edge peak energy corresponds to the energy difference between the 1s level and the unoccupied 3d levels of center ions, the latter of which are influenced by the ligand field [26–28]. The higher pre-edge energy (at 6542.2 eV) for the **1**/MK10 hybrid could be explained by an increase of the unoccupied 3d levels, possibly due to a distorted local coordination structure of Mn ions. However, it is also established that pre-edge peak energy depends on the valence state of the center ions; pre-edge peak energy shifts to higher energy with an increase in the oxidation number of iron [29–31] and manganese [32]. The possible explanation by the higher valence state could not be excluded for the higher pre-edge energy of the **1**/MK 10 hybrid.

The amount of O_2 evolved in the reaction of neat **1** or the **1**/MK10 hybrid with a large excess Ce^{IV} oxidant in an aqueous solution or suspension was measured. In the solution of neat **1**, the reaction did not produce O_2 at all (Fig. 3a). The absorption spectroscopic measurements indicated that the reaction leads to decomposition of **1** to MnO_4^- ions possibly by disproportionation. However, it can be significantly suppressed by adsorption of **1** onto MK10 [33]. The reaction of the **1**/MK10 hybrid produced a significant amount of O_2 (Fig. 3c), in contrast to no O_2 evolution for neat **1** in solution. O_2 evolution was not observed when using MK10 without **1** as a control (Fig. 3d), showing that O_2 is evolved by **1** adsorbed on MK10. The amount (n_{O2}/mol) of O_2 evolved under the conditions (**1**, 1.0 μmol; MK10, 20 mg; Ce^{IV}, 1 mmol; liquid volume, 2 ml) was 6.5 μmol, corresponding to 6.5 of turnover number (TN) of **1** for O_2 evolution. This result shows that **1** adsorbed on MK10 catalyzes O_2 evolution. The ^{18}O-labeling O_2 evolution experiments corroborated that the oxygen atoms for O_2 evolution are exclusively originated from water [21].

2 has comparable structure with **1** but no terminal water ligands. The same O_2 evolution experiments were carried out using **2** in solution and on MK10 to compare with the reactions of **1**. In the solution of neat **2**, the reaction with Ce^{IV} did not produce O_2, but led to decomposition to MnO_4^- ions similar to neat **1** in solution. For **2**/MK10, O_2 was evolved by the reaction with Ce^{IV}. However, the TN value was less than unity for **2**/MK10 (TN=0.35) under the same conditions as **1**/MK10 (**2**, 1.0 μmol; MK10, 20 mg; Ce^{IV}, 1 mmol; liquid volume, 2 ml). This result shows that **2** adsorbed on MK10 does not work as a catalyst. The terminally coordinated water ligands could be an important for the catalysis by adsorbed **1**.

The initial O_2 evolution rate (v_{O2}/mol s^{-1}) was calculated from the initial slope of the time course. The v_{O2} for **1**/MK10 and **2**/MK10 were plotted vs. the amount (n_{ads}) of **1** or **2** adsorbed on MK10 in Fig. 4, including v_{O2} data for **1**/kaolin and **2**/kaolin for comparison. The plots for **1**/MK10 (Fig. 4a) and **1**/kaolin (Fig. 4c) gave upward curves at respective low n_{ads} regions, and they departed from the upward curvature above n_{ads}=6.0 and 0.9 μmol for **1**/MK10 and **1**/kaolin, respectively. This departure is ascribed to elution of **1** from MK10 and kaolin into the liquid phase to promote decomposition of **1** to MnO_4^- ions. The upward curvature in the v_{O2} vs. n_{ads} plots is in contrast to the linear plots for **2**/MK10 (Fig. 4b) and **2**/kaolin (Fig. 4d) showing the first order O_2 evolution with respect to **2**.

v_{O2} was analyzed by the kinetic model (Eq. (2)) assuming on combination between first and second order O_2 evolutions with respect to adsorbed **1**:

$$v_{O2} = k_1 n_{ads} + k_2 n_{ads}^2 \quad (2)$$

where k_1/s^{-1} and k_2/mol^{-1} s^{-1} are first order and second order rate constants for O_2 evolution, respectively. For comparing the turnover frequency of **1** adsorbed on MK10, v_{O2} was normalized by n_{ads} to define the apparent turnover frequency,

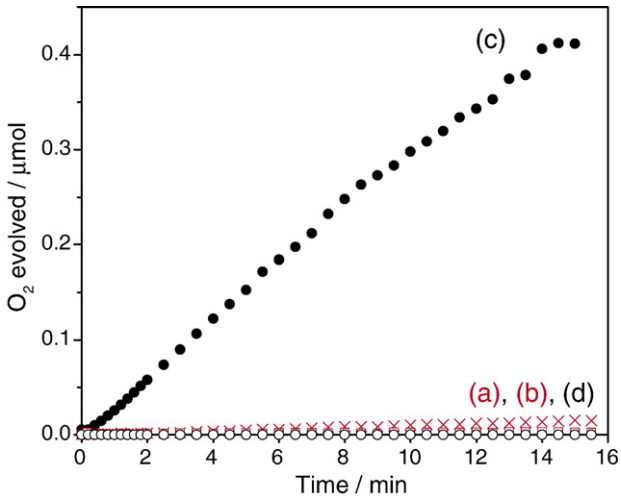

Fig. 3. Time courses of the amount of O_2 evolved in reactions of **1** and a 50 mM Ce^{IV} oxidant. (a) Aqueous solution of **1** (2.0 μmol; 1.0 mM) (□), (b) aqueous solution without **1** (×), (c) aqueous suspension of MK10 (75 mg) adsorbing 2.0 μmol **1** (w_{ads}=27 μmol g^{-1}) (●) and (d) aqueous suspension of MK10 (75 mg) without **1** (○). Liquid volume, 2.0 ml; pH=1.0.

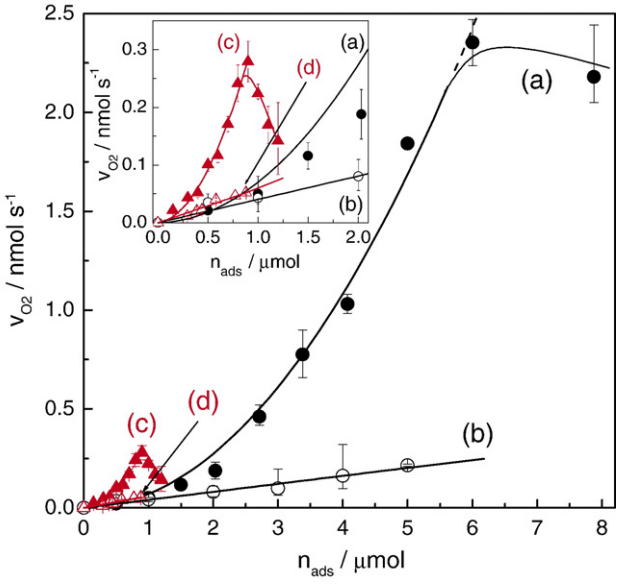

Fig. 4. Plots of initial rate (v_{O2}/mol s^{-1}) of O_2 evolution vs. the amount (n_{ads}) of **1** or **2** for (a) **1**/MK10, (b) **2**/MK10, (c) **1**/kaolin and (d) **2**/kaolin. 50 mM Ce^{IV}; liquid volume, 2.0 ml; pH = 1.0. The inset shows the magnified figure for kaolin systems. Some v_{O2} data for (c) **1**/kaolin and (d) **2**/kaolin were partially cited from reference [21].

$(k_{O2})_{app}/s^{-1}$ as Eq. (3). The plots of $(k_{O2})_{app}$ vs. n_{ads} can provide k_1 and k_2 from the intercept and the slope, respectively.

$$(k_{O2})_{app} = v_{O2}/n_{ads} = k_1 + k_2 n_{ads} \quad (3)$$

For **1**/MK10 and **1**/kaolin, the plots of $(k_{O2})_{app}$ vs. n_{ads} gave the straight lines with significant slopes passing through the near origin at $n_{ads} < 6.0$ μmol and at $n_{ads} < 0.9$ μmol, respectively, as shown in Fig. 5. The significant slope and the almost zero intercept suggest that O_2 is predominantly evolved by a bimolecular reaction of adsorbed **1**. The best fitting of Eq. (3) to the $(k_{O2})_{app}$ data yielded k_1 and k_2 values summarized in Table 1. The k_1 values are close between **2**/MK10 and **2**/kaolin, whereas the k_2 value (3.2×10^2 mol^{-1} s^{-1}) for **1**/kaolin is 4.9 times higher than that (6.5×10 mol^{-1} s^{-1}) for **1**/MK10. This result shows that second order O_2 evolution strongly depends on the clay matrix though first order one is almost independent of it. The higher k_2 for **1**/kaolin can be explained by localized adsorption of **1** on the kaolin surface. For the XRD pattern of MK10 any intense peak cannot be observed in the range of $2\theta = 0$–15 degree, which is consistent with a card house structure of MK10. **1** is supported to be adsorbed in an interlayer of the card house structure. The XRD pattern of kaolin, exhibiting an intense sharp peak at $2\theta = 12.4$ degree, did not change by adsorption of **1**, suggesting that **1** is adsorbed onto the surface of kaolin. This results in a localization of **1** on the kaolin surface, making cooperative interaction for O_2 evolution easier.

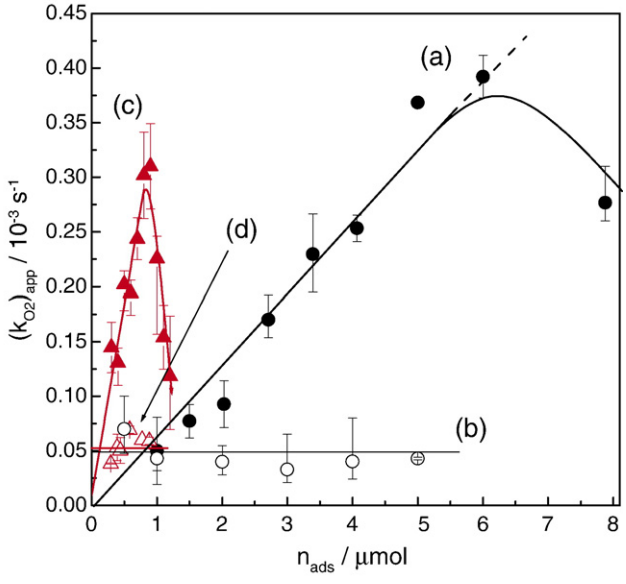

Fig. 5. Plots of $(k_{O2})_{app}$ vs. the amount (n_{ads}) of **1** or **2** for (a) **1**/MK10, (b) **2**/MK10, (c) **1**/kaolin and (d) **2**/kaolin. The conditions were indicated in Fig. 4.

Table 1
Summary of k_1 and k_2

Complex	Clay	Rate constant	
		k_1 (s^{-1})	k_2 (mol^{-1} s^{-1})
1	kaolin	–	$3.2\ (\pm 0.6) \times 10^2$
	MK10	–	$6.5\ (\pm 0.5) \times 10$
2	kaolin	$5.9\ (\pm 0.3) \times 10^{-5}$	–
	MK10	$4.0\ (\pm 0.2) \times 10^{-5}$	–

4. Discussion

The first order O_2 evolution by **2** adsorbed on MK10 could involve decomposition because **2** does not work as a catalyst. It might be explained by either O − O coupling of di-μ-O bridges or attack of outer-sphere water onto a μ-O bridge in high oxidation species, probably including μ-O$^{\bullet}$ radical bridges. A coupling of di-μ-O$^{\bullet}$ radical bridges in a $Mn(\mu\text{-}O)_2Mn$ unit was proposed by Yachandra et al. as a possible mechanism of O_2 production in OEC taking a hint from EXAFS data [1]. Although the di-μ-O bridges must be activated by adsorbing onto the MK10 for O_2 evolution, the activation mechanism is still under consideration.

The second order O_2 evolution catalyzed by **1** adsorbed on MK10 suggests that cooperation of two equivalents of **1** is required for the catalysis. The adsorption of **1** onto MK10 results in its higher concentration than that in its solution, making the cooperative interaction for the catalysis easier. The k_2 values that are strongly dependent on the clay matrix could support the cooperative interaction. The non-catalytic activity and the first order O_2 evolution by **2** imply that the terminal water ligand on **1** is involved for catalysis. The O_2 evolution may take place by intermolecular coupling of oxo groups on Mn ions that could be originated from terminal water ligands on **1**. The detailed spectroscopic measurements will be needed to identify the key oxo group on the Mn ion involved in O − O bond formation.

The present O_2 evolution catalyzed by **1** adsorbed on MK10 might give some insights into the O_2 evolution mechanism by OEC. The cooperative catalysis by two equivalents of **1** might imply that, for O_2 production by OEC, an O − O bond is formed by coupling of oxos coordinated on Mn ions rather than attack of outer-sphere water onto an oxo coordinated on a Mn ion. The orientation of oxos on Mn ions and distance between them might be precisely controlled by proteins for OEC, contrasting with the present artificial model in which the cooperative interaction is randomly supported by MK10. The catalysis by **1** on MK10 does not need a Ca^{2+} ion. The possibility is given that Ca^{2+} may play a role in photoactivation or incorporation of water substrate to the Mn cluster, rather than be directly involved in O − O bonding formation for OEC.

5. Conclusion

The artificial model of photosynthetic OEC was yielded by adsorption of **1** onto MK10. The present paper illustrates evidence of catalytic O_2 evolution from water by **1** adsorbed on MK10. The kinetic analysis suggested that O_2 evolution occurs by a bimolecular reaction of **1** adsorbed on MK10. It requires cooperative interaction of two equivalents of **1** adsorbed. The mechanism of O − O bond formation was hypothesized to involve intermolecular coupling of oxo groups on Mn ions that could be originated from the terminal water ligands on **1** in the O_2 evolution. O_2 evolution by **2** adsorbed on MK10 was a first order reaction with respect to **2**. However, it did not work as a catalyst. Insight into the O_2 evolution mechanism by OEC was provided based on catalytic O_2 evolution by **1** on MK10.

Acknowledgments

The research was supported by Grant-in-Aid for Young Scientists (B) from the Ministry of Education, Culture, Sports, Science and Technology (No. 16750113). The X-ray absorption experiments were performed under the approval of the Photon Factory Program Advisory Committee (Proposal No. 2005G189).

References

[1] V.K. Yachandra, K. Sauer, M.P. Klein, Manganese cluster in photosynthesis: where plants oxidize water to dioxygen, Chem. Rev. 96 (1996) 2927–2950.

[2] T.G. Carrell, A.M. Tyryshkin, G.C. Dismukes, An evaluation of structural models for the photosynthetic water-oxidizing complex derived from spectroscopic and X-ray diffraction signatures, J. Biol. Inorg. Chem. 7 (2002) 2–22.

[3] A. Zouni, H.T. Witt, J. Kern, P. Fromme, N. Krauss, W. Saenger, P. Orth, Crystal structure of photosystem II from *Synechococcus elongatus* at 3.8 angstrom resolution, Nature 409 (2001) 739–743.

[4] J. Nugent (Ed.), "Photosynthetic Water Oxidation" special issue, Biochim. Biophys. Acta-Bioenerg., vol. 1503, 2001.

[5] K.N. Ferreira, T.M. Iverson, K. Maghlaoui, J. Barber, S. Iwata, Architecture of the photosynthetic oxygen-evolving center, Science 303 (2004) 1831–1838.

[6] B. Loll, J. Kern, W. Saenger, A. Zouni, J. Biesiadka, Towards complete cofactor arrangement in the 3.0 Å resolution structure of photosystem II, Nature 438 (2005) 1040–1044.

[7] R. Ramaraj, A. Kira, M. Kaneko, Oxygen evolution by water oxidation mediated by heterogeneous manganese complexes, Angew. Chem., Int. Ed. Engl. 25 (1986) 825–827.

[8] R. Ramaraj, A. Kira, M. Kaneko, Heterogeneous water oxidation by a dinuclear manganese complex, Chem. Lett. (1987) 261–264.

[9] M. Yagi, M. Kaneko, Molecular catalysts for water oxidation, Chem. Rev. 101 (2001) 21–35.

[10] W. Ruettinger, G.C. Dismukes, Synthetic water-oxidation catalysts for artificial photosynthetic water oxidation, Chem. Rev. 97 (1997) 1–24.

[11] W. Ruettinger, M. Yagi, K. Wolf, S. Bernasek, G.C. Dismukes, O_2 evolution from the manganese-oxo cubane core $Mn_4O_4^{6+}$: a molecular mimic of the photosynthetic water oxidation enzyme? J. Am. Chem. Soc. 122 (2000) 10353–10357.

[12] M. Yagi, K.V. Wolf, P.J. Baesjou, S.L. Bernasek, G.C. Dismukes, Selective photoproduction of O_2 from the Mn_4O_4 cubane core: a structural and functional model for the photosynthetic water-oxidizing complex, Angew. Chem., Int. Ed. 40 (2001) 2925–2928.

[13] J. Limburg, J.S. Vrettos, L.M. Liable-Sands, A.L. Rheingold, R.H. Crabtree, G.W. Brudvig, A functional model for O−O bond formation by the O_2-evolving complex in photosystem II, Science 283 (1999) 1524–1527.

[14] J. Limburg, J.S. Vrettos, H.Y. Chen, J.C. de Paula, R.H. Crabtree, G.W. Brudvig, Characterization of the O_2-evolving reaction catalyzed by $[(terpy)(H_2O)Mn^{III}O_2Mn^{IV}(OH_2)(terpy)](NO_3)_3$ (terpy=2,2′:6,2″-terpyridine), J. Am. Chem. Soc. 123 (2001) 423–430.

[15] Y. Naruta, M. Sasayama, T. Sasaki, Oxygen evolution by oxidation of water with manganese porphyrin dimers, Angew. Chem., Int. Ed. Engl. 33 (1994) 1839–1841.

[16] Y. Shimazaki, T. Nagano, H. Takesue, B.-H. Ye, F. Tani, Y. Naruta, Characterization of a dinuclear $Mn^{V}O$ complex and its efficient evolution of O_2 in the presence of water, Angew. Chem., Int. Ed. 43 (2004) 98–100.

[17] H. Chen, R. Tagore, S. Das, C. Incarvito, J.W. Faller, R.H. Crabtree, G.W. Brudvig, General synthesis of di-μ-oxo dimanganese complexes as functional models for the oxygen evolving complex of photosystem II, Inorg. Chem. 44 (2005) 7661–7670.

[18] H. Chen, J.W. Faller, R.H. Crabtree, G.W. Brudvig, Dimer-of-dimers model for the oxygen-evolving complex of photosystem II. Synthesis and properties of $[Mn_4^{IV}O_5(terpy)_4(H_2O)_2](ClO_4)_6$, J. Am. Chem. Soc. 126 (2004) 7345–7349.

[19] C. Baffert, S. Romain, A. Richardot, J.-C. Lepretre, B. Lefebvre, A. Deronzier, M.-N. Collomb, Electrochemical and chemical formation of $[Mn_4^{IV}O_5(terpy)_4(H_2O)_2]^{6+}$, in relation with the photosystem II oxygen-evolving center model $[Mn_2^{III,IV}O_2(terpy)_2(H_2O)_2]^{3+}$, J. Am. Chem. Soc. 127 (2005) 13694–13704.

[20] H. Wolpher, P. Huang, M. Borgstroem, J. Bergquist, S. Styring, L. Sun, B. Akermark, Synthesis of a $Ru(bpy)_3$-type complex linked to a free terpyridine ligand and its use for preparation of polynuclear bimetallic complexes, Catal. Today 98 (2004) 529–536.

[21] M. Yagi, K. Narita, Catalytic O_2 evolution from water induced by adsorption of $[(OH_2)(terpy)Mn(\mu\text{-}O)_2Mn(terpy)(OH_2)]^{3+}$ complex onto clay compounds, J. Am. Chem. Soc. 126 (2004) 8084–8085.

[22] S.R. Cooper, M. Calvin, Mixed valence interactions in di-μ-oxo bridged manganese complexes, J. Am. Chem. Soc. 99 (1977) 6623–6630.

[23] K. Narita, Studies on catalytic O_2 production from water induced by adsorption of dinuclear Mn complexes onto heterogeneous solid matrixes, Master's thesis, Niigata University (2004).

[24] J.H. Clark, S.R. Cullen, S.J. Barlow, T.W. Bastock, Environmentally friendly chemistry using supported reagent catalysts: structure–property relationships for clayzic, J. Chem. Soc., Perkin Trans. 2 (1994) 1117–1130.

[25] H. Visser, E. Anxolabe, U. Lhe`re-Mallart, P. Bergmann, J.H. Glatzel, S.P. Robblee, J.-J. Cramer, K. Girerd, M.P. Sauer, V.K. Klein, Mn K-Edge XANES and Ka XES studies of two Mn-oxo binuclear complexes: investigation of three different oxidation states relevant to the oxygen-evolving complex of photosystem II, J. Am. Chem. Soc. 123 (2001) 7031–7039.

[26] K. Shimizu, H. Maeshima, H. Yoshida, A. Satsuma, T. Hattori, Ligand field effect on the chemical shift in XANES spectra of Cu(II) compounds, Phys. Chem. Chem. Phys. 3 (2001) 862–866.
[27] S.J. George, M.D. Lowery, E.I. Solomon, S.P. Cramer, Copper L-edge spectral studies: a direct experimental probe of the ground-state covalency in the blue copper site in plastocyanin, J. Am. Chem. Soc. 115 (1993) 2968–2969.
[28] F. Farges, E. Brown, J.J. Rehr, Ti K-edge XANES studies of Ti coordination and disorder in oxide compounds: comparison between theory and experiment, Phys. Rev. B 56 (1997) 1809–1819.
[29] C.A. Linkous, W.E. O'Grady, D. Sayers, C.Y. Yang, Spectrophotometric and X-ray absorption edge study of complexation of carbon monoxide with ferric tetrasulfophthalocyanine in alkaline solution, Inorg. Chem. 25 (1986) 3761–3765.
[30] T.E. Westre, P. Kennepohl, J.G. DeWitt, B. Hedman, K.O. Hodgson, E.I. Solomon, A multiplet analysis of Fe K-Edge 1s 3d pre-edge features of iron complexes, J. Am. Chem. Soc. 119 (1997) 6297–6314.
[31] A.L. Roe, D.J. Schneider, R.J. Mayer, J.W. Pyrz, J. Widom, L. Que, X-ray absorption spectroscopy of iron-tyrosinate proteins, J. Am. Chem. Soc. 106 (1984) 1676–1681.
[32] M. Kusunoki, O. Taka-ki, T. Matsushita, H. Oyanagi, Y. Inoue, Mn K-edge XANES spectroscopy of a photosynthetic O_2-evolving complex. High-quality pre-edge features and distinct fine structures in the S_1- and S_2-States1, J. Biochem. 108 (1990) 560–567.
[33] The MnO_4^- ions formed were also observed in the liquid phase for the **1**/MK10 hybrid. The yields (18.3–31.3%) of MnO_4^- for the **1**/MK10 hybrid were significantly less than that (56.3–85.8%) in the solution under the comparable conditions.